DR JUDIT MOLERA (Orcid ID : 0000-0003-3116-0456)

PROFESSOR TRINITAT PRADELL (Orcid ID : 0000-0002-8720-5492)

Article type : Article

Corresponding Author mail id:-judit.molera@uvic.cat

The production of a lead glaze with galena: thermal transformations in the PbS-SiO_2 system

Roberta Di Febo[1], Judit Molera[1], Trinitat Pradell[2], Joan Carles Merlgarejo[3], Josep Madrenas[4], Oriol Vallcorba[5]

[1]U. Science Tech, MECAMAT group, University of Vic-Central University of Catalonia-, de la Laura 13, 08500, Vic, Catalonia

[2]Physics Department, UPC-BarcelonaTech, campus Baix Llobregat, Esteve Terrades 8, 08860, Castelldefels, Catalonia

[3]Dpt. Mineralogia, Petrologia i Geologia Aplicada, University of Barcelona, Martí i Franquès, s/n - 08028 Barcelona, Catalonia

[4] Escola d'Art i Superior de Disseny de Vic, Rambla de Sant Domènec, 24, 08500, Vic, Catalonia

[5]ALBA Synchrotron Light Source, Cerdanyola del Vallès, 08290, Barcelona, Catalonia

Abstract

Galena, also known as PbS, was widely used in the production of lead glazes from the beginning of the 18th century to the second half of the 20th century. Although the SiO_2-PbO system has been studied for years, the PbS-SiO_2 phase diagram, involved in the formation of a glaze with galena, has not yet been investigated. Temperature transformations for the system 75 wt. % PbS – 25 wt. % SiO_2 are investigated in a high temperature resolved X-ray Diffraction experiment with Synchrotron Radiation (HT-SR-XRD) and compared to those of the equivalent system 70 wt. % PbO – 30 wt. % SiO_2. Lanarkite, $PbO·PbSO_4$, is the phase predominantly formed as soon as galena decomposes during the heating. The results show that the system

This article has been accepted for publication and undergone full peer review but has not been through the copyediting, typesetting, pagination and proofreading process, which may lead to differences between this version and the Version of Record. Please cite this article as doi: 10.1111/jace.15346

melts at a temperature higher than the $PbO-SiO_2$ system, but far lower than those expected for the $PbO-PbSO_4-PbS$ system. A historical misfired lead glaze produced with galena is also studied. The presence of galena, lanarkite and mattheddleite $Pb_{10}(SiO_4)_{3.5}(SO_4)_2Cl_2$, is determined and discussed in terms of the composition of the galena mineral used and the firing conditions in light of the high temperature transformations previously obtained.

KEYWORDS: $PbS-SiO_2$ system, $PbO-SiO_2$ system, galena, $PbO{\cdot}PbSO_4$ lanarkite, $2PbO{\cdot}PbSO_4$, $4PbO{\cdot}PbSO_4$ mattheddleite, high lead glazes, thermal stability

I. Introduction

Lead glazes are among the earliest glazes used to coat earthenware, stoneware and porcelain to make them waterproof. Lead glazes have a wide processing range, low meting point, low viscosity and surface tension and a thermal expansion coefficient which match those of earthenware giving them good adherence (minimal flaking and crazing) and excellent covering capability. They also have a high refraction index that confers brilliance to the glaze.[1]

The first lead containing glazes were produced in China (Warring states period, 475-221 BC), to cover large jars, but were comprised of relatively low quantities of lead (<20 wt. % PbO). High lead glazes (with composition close to the eutectic mixture 70 wt. % PbO, 30 wt. % SiO_2, which melts at 717º C) were not produced until the 1st century BC (Han dynasty and Greco-Roman world) [2-3]. All these glazes show green, yellow and brown colours and imitated metal forms.[4]

There were two primary methods of applying lead glazes to ceramic surfaces: either by using lead compounds alone or a mixture of lead compounds plus powdered quartz or sand[2]. The former method was used between the 1st and 3rd centuries AD and the latter between the 2nd and 4th centuries AD[4]. One further variation was the *fritting* of the lead compounds-plus-quartz mixture before its application to the ceramic surface.[1] A *frit* is any glassy or partially glassy material obtained after firing a mixture of sand with flux materials (lead compounds, plant ashes, alkaline salts, etc)[5]. This method was widely used in the Medieval period until modern times.

Galena, PbS, is the most important lead ore, and known to have been widely exploited by the Romans to extract silver and to obtain metallic lead, but there is no archaeological evidence or literature demonstrating the use of galena or roasted galena (PbO) in the production of the lead glaze in Roman times. The use of galena would have the advantage of eliminating one stage (the roasting of galena to obtain lead oxide) in the process of producing a lead glaze. However, the use of galena was not documented until the 18th century[6]. At the same time as Ramazzini, an Italian physician, linked the diseases shared by potters, guilders and glass makers to lead poisoning.[7]

Although there is a detailed phase diagram for the PbO-SiO_2 system [8,9,10], there is no information about the transformations that take place in the PbS-SiO_2 system. However, complementary information of the Pb-PbS, PbS-O and PbO-$PbSO_4$ systems is available[11-14]. The use of *galena* implies the oxidation of PbS, but as PbS and PbO do not have a common boundary in the phase diagram, it will always involve the formation of lead sulphates and oxysulphates; PbO·$PbSO_4$, 2PbO·$PbSO_4$, 4PbO·$PbSO_4$ which are known to have a limited solubility in the silica melt. Therefore, the use of *galena* implies oxidation of the PbS into $PbSO_4$ and progressively more oxidised oxysulphates, sulphate anion breakdown (above 880º C) and the reaction with SiO_2 to obtain the melt. The main advantage of the PbO-SiO_2 system in the production of glazes is its low melting point (717º C[10]). The large compositional range, between 20 and 60 mol. % SiO_2, for which a melt forms at a relatively low temperature, below 760º C[10] is also an advantage. This does not occur in the PbS-SiO_2 system. The PbS-$PbSO_4$-PbO phase diagrams show higher melting temperatures, the lowest for the more oxidised species at 916º C.

The production of a lead glaze with *galena*, PbS-SiO_2 system, and the equivalent PbO-SiO_2 system are investigated in a time resolved high temperature X-ray Diffraction experiment with Synchrotron Radiation (HT-SR-XRD). Although the equilibrium phase diagram of the PbO-SiO_2 system is well known, equilibrium conditions are not necessarily reached during the time resolved experiment. Therefore, the data obtained for the PbO-SiO_2 mixture will reveal any shift in the phase transformation and melting temperatures due to non-equilibrium conditions.

A historical misfired lead glaze ware that retains *galena* relic grains is also studied. The crystalline phases present in the glaze vestiges from an incomplete glaze firing are identified and their presence discussed in terms of the data obtained from the High temperature experiment and of the composition of the glaze. Finally, the reasons for the use of galena in the production of lead glazes and its limitations are discussed in light of the results obtained.

II. Experimental Procedure

(1) High-temperature resolved XRD experiment (HT-SR-XRD)

Two mixtures of the eutectic composition 70 wt. % PbO : 30 wt. % SiO_2 were prepared using PbO in one case and using galena in the second case. Chemical reagents for both the PbO (Fluka ref. 11526) and SiO_2 (Merck ref. 107536) were selected. Galena is of mineral origin and the sample obtained was from the Molar mine (Catalonia).

The *in situ* high-temperature X-ray diffraction measurements were obtained on the high-brilliance, high-energy (90 keV) synchrotron beamline ID15B at the ESRF (Grenoble, France). The experimental setup consisted of a small cylindrical furnace with the raw powders contained in unsealed 0.5-mm-diameter MgO capillaries mounted on a goniometer for alignment. An image-plate detector (Model MAR345, Marresearch, Norderstedt, Germany) was used to collect the XRD patterns with an exposure time of 1 min and rotation of the sample was sufficient to ensure good data quality.

The furnace temperature was controlled by a previously calibrated external regulator. An initial drying stage was programmed, consisting of a slow heating rate (1°C/min) between 90°–110°C and then maintaining the temperature for 5 minutes. The sample was afterwards heated at a constant heating rate of 5°C/min up to the maximum temperature with data being recorded during this slow ramping. The measuring time took only 1 min and consequently a variation of 5°C existed between the beginning and the end of the data collection. The data collection, readout, and erasure of the image-plate took 4 min in total. The whole cycle for each dataset took 5 min (measuring time, readout, and then erasure of the image plate), resulting in images being taken every 25°C. Finally, the sample was cooled down to room temperature at a rate of 10°C/min. The whole measurement cycle took 3h.

The calibration of the sample to detector distance, beam centre and orthogonality of the detector were determined using a silicon standard measured under the same conditions. The radial integration of the images was performed using the Fit2D software.[15] Identification of the compounds was performed based on the Powder Diffraction File (PDF) database from the International Centre for Diffraction Data (ICDD). Fig. 2 and 3 represents high temperature XRD patterns (HT-SR-XRD) obtained during the firing of the mixtures. Thermal stability ranges of the crystalline phases identified for (a) PbO-SiO_2 and (b) PbS-SiO_2 are shown in Figure 4. The ordinate axis is obtained from the intensity of the principal peak of each crystalline phase relative to the intensity of the MgO crucible, and gives a qualitative temperature evolution of each compound.

(2) Analysis of a misfired lead glaze

A misfired storage jar (CCV050) dating from the 18th century was investigated[6]. The jar was part of an assemblage of coarse wares found in the garret of *Casa Convalescència*, an ancient hospital building that provided medical assistance, in Vic. Due to uncontrolled and unequal temperature conditions in the kiln, the glaze exhibits three different colours: opaque green, opalescent yellow and transparent honey (*Figure 1*).

A polished thin section of glaze and ceramic body to a standard thickness of 30 µm was obtained. The thin section was studied by Optical Microscopy (OM) with transmitted and reflected light using a petrographic microscope (LEICA DM 2700 P) and Scanning Electron Microscopy with an Energy Dispersive Spectroscopy detector attached (SEM-EDS) to identify the crystalline compounds present. A crossbeam workstation (Zeiss Neon 40) equipped with a Shottky Field emitter column with an EDS detector (INCAPentaFETx3 detector, 30 mm^2, ATW2 window) attached was employed for the SEM investigation. Backscattered electron (BSE) images were obtained and analyses of the crystallites were carried out to ascertain the composition at 20 kV acceleration voltage.

Electron Microprobe (EPM, JEOL JXA-8230) was also used to quantify the chemical composition of the different micro-crystallites present that contained both Pb and S which requires the high energy resolution provided by the WDS (wavelength dispersive spectroscopy) detector. A minimum of three analyses of the crystallites and of the glaze were acquired and the average and standard deviation were obtained. The operating conditions were 20 kV and 15nA with a focused beam (spot analysis). The standards used were PbS for galena and Pb, $SrSO_4$ for S, $CaSiO_3$ for Si and Ca and AgCl for Cl. Finally, the chemical composition of the glaze was determined avoiding the glaze-ceramic interface as well as the crystallites.

The crystalline structure of the micro-crystallites was determined by Synchrotron Radiation micro-X-ray diffraction (SR-μXRD) on the same polished thin section in the focused-beam station of beamline BL04[16] at the ALBA Synchrotron (Spain). The areas of interest from the polished thin section were selected using an on-axis visualization system and measured in transmission geometry with a 15x15 μm^2 (FWHM) focused beam of 29.2 KeV (λ = 0.4246 Å). The diffraction patterns were recorded with a Rayonix SX165 CCD detector (active area of 165mm diameter, frame size 2048 x 2048 pixels, 79µm pixel size, dynamic range 16 bit). The calibration of the sample to detector distance, beam centre and orthogonality of the detector was performed using a LaB_6 standard and the radial integration of the images was performed with the Fit2D software.[15] Identification of the compounds was performed based on the Powder Diffraction File (PDF) database from the International Centre for Diffraction Data (ICDD).

III. Results

The corresponding high temperature diffraction data taken during the heating of PbO-SiO_2 and PbS-SiO_2 mixtures are shown in 2D images in *Figure 2* and *Figure 3* respectively. The HT-SR-XRD patterns taken before heating and after cooling are also shown. Apart from the initial and new crystalline compounds formed during the heating, the XRD pattern corresponding to the periclase (MgO) from the crucible is also seen.

(1) PbO-SiO_2 high-temperature resolved XRD experiment

The high temperature diffraction data taken during the heating of a mixture 70 wt. % PbO : 30 wt. % SiO_2 is shown in *Figure 2* and the appearance and disappearance of the phases marked. The initial compounds are massicot (PbO, orthorhombic, Pbcm) and α-quartz (SiO_2, trigonal). The thermal stability range of the different compounds identified is summarised in *Figure 4a.*

The reversible transformation between α-SiO_2 and β-SiO_2 at 573º C, is observed in *Figure 2*. PbO was stable up to 560º C. At 600º C, PbO began to decrease until it disappeared completely at 722º C. A melt coexisting with other crystalline compounds (a melt is expected to form at 717º C[10] in the system 70 wt. % PbO – 30 wt. % SiO_2) was clearly found at about 722º C. As soon as PbO reacted with SiO_2, Pb_2SiO_4 was formed increasing until 690º C; it decreased quickly at 715º C and completely disappeared at 727º C. At 670º C Pb_4SiO_6 was formed and disappeared at 722º C. Finally, $PbSiO_3$ was formed at 625º C and disappeared completely at 727º C with an increase in the range 715-722º C, just when Pb_4SiO_6 decomposed incongruently into Pb_2SiO_4 and $PbSiO_3$.

(2) High-temperature resolved XRD experiment PbS-SiO$_2$

The high temperature diffraction data obtained for a mixture of 75 wt. % of galena plus 30 wt. % of quartz with a composition equivalent to the eutectic composition 70 wt. % PbO : 30 wt. % SiO_2 is shown in *Figure 3.* The appearance and disappearance of the phases are also marked. The initial compounds determined were galena (PbS), α-quartz, anglesite ($PbSO_4$), cerussite ($PbCO_3$) as well as periclase (MgO) from the crucible. Both anglesite and cerussite are weathering compounds of the natural galena deposit, and were present in a very small amount. The thermal stability ranges of the crystalline phases identified is summarised in *Figure 4b.*

Galena was stable up to 315º C and then began to slowly decrease until it disappears completely at 795º C. A melt coexisting with other crystalline compounds appeared at about 775º C (a melt is expected at 717º C in the system 70 wt. % PbO – 30 wt. % SiO_2)[10]. With regard to the galena weathering compounds, cerussite was stable up to 275º C decreasing from 275º C upwards and disappearing at 315º C. Massicot (PbO) appeared at 315º C increasing up to 475º C and completely disappearing at 595º C. Anglesite was stable up to 575º C, increasing between 575º C and 775º C and afterwards decreasing when it completely disappeared at 860º C. The reversible transformation between α-$PbSO_4$ and β-$PbSO_4$ at 883º C did not occur because the anglesite had already fully decomposed at a lower temperature (≈860º C) in our system. The appearance of lead oxy-sulphate, $PbO \cdot PbSO_4$ (lanarkite)[17], followed the decrease of galena (above 315º C) increasing progressively, but more quickly between 595º C and 775º C. Lanarkite suddenly disappeared at 795º C and a lead dioxy-sulphate, $2PbO \cdot PbSO_4$ formed. The lead dioxy-sulphate, $2PbO \cdot PbSO_4$ began to decrease at 900º C completely disappearing at 950º C. Minium (Pb_3O_4) formed between 810º C and 860º C and was not found at 900º C. Meanwhile a second melt developed; in fact, according to the PbO-$PbSO_4$ phase diagram a sulphate melt should appear at this temperature[13]. At 900º C forsterite (Mg_2SiO_4) was also formed due to the reaction of the silica melt with the magnesia crucible. After cooling, the crystalline phases found were $2PbO \cdot PbSO_4$ and $4PbO \cdot PbSO_4$ -crystallising from the sulphate melt-, quartz and forsterite (Mg_2SiO_4).

In summary, the oxidation of galena (*Figures 4 and 5*) gave rise mainly to the formation of lanarkite, anglesite and $2PbO \cdot PbSO_4$. In theory anglesite is the first phase formed during the oxidation of galena[11]. However, this is only true at very low temperatures. According to other studies[14], lanarkite is actually the phase predominantly formed during the roasting of galena at 600º C[6]. In our case, the anglesite determined was, in fact, already present in the original galena ore although some was also formed during the decomposition of galena between 600º C and 800º C. The PbO-$PbSO_4$ phase diagram[11] indicates that both $PbSO_4$ and PbO·$PbSO_4$, are stable at temperatures below 928º C when a sulphate liquid is formed. In contrast, in our case, a PbO-SiO_2 melt already developed at a lower temperature, ~775º C and anglesite disappeared completely at ~860º C. In addition, the PbO-$PbSO_4$ phase diagram also indicates that, on further oxidation, lanarkite and 2PbO·$PbSO_4$ should coexist. However, in our case, lanarkite decomposed completely at 795º C while the lead dioxy-sulphate 2PbO·$PbSO_4$ was formed which in turn decomposed at 950º C when a melt was formed. During the cooling, two lead oxy-sulphates, 2PbO·$PbSO_4$ and 4PbO·$PbSO_4$ recrystallized from the melt; this is consistent with the PbO-$PbSO_4$ phase diagram where both compounds are stable below 863º C.[11] In fact, the presence of these lead oxy-sulphates indicates that a complete oxidation of galena into PbO was not obtained during the heating.

(3) Analysis of a misfired lead glaze

The misfired lead glaze exhibits three distinctive areas of different colours: opaque green, opalescent yellowish and transparent honey, *Figure 1*. *Figure 1 (a-c)* shows SEM BSE images corresponding to the green, yellow and honey coloured areas respectively. Three types of crystallites are observed in the three areas and all of them contain mainly Pb and S (*Figure 1d*). Type I crystals appearing light grey are found only in the green glaze, *Figure 1(a).* Type II crystals, which appear slightly darker in the SEM BSE images, show tabular or elongated sections of euhedral crystals. They also have a similar composition to Type I crystals, *Figure 1(d)* and are found in both the green and the yellow glazes, *Figure 1(a,b)*. Type III crystals show a similar light grey colour and share the tabular or elongated sections of euhedral crystals as found in Type II. They are present in the three coloured areas of the glaze, *Figure 1*. However, the chemical composition of Type III crystals is slightly different to those of Type II; they contain mainly Pb and S. but also some Cl, and minor amounts of Si and Ca, *Figure 1(d)*. Crystallites, Type II and Type III, show a similar atomic contrast in the BSE images. Quantitative chemical analysis of the crystallites is not possible with the EDS detector because of the large overlapping of S-Kα, Pb-Mα and Cl-Kα X-ray fluorescent peaks. Consequently, the chemical composition of the crystallites and the glaze is obtained by EPM, using a Wavelength Dispersive X-ray Spectroscopy detector system (WDS) with a superior X-ray peak resolution and greater peak to background ratio. The chemical composition of the glaze in wt. % is 73.5 % PbO, 19.6 % SiO_2, 1.5 % Al_2O_3, 1.5 % SO_3, 1.2 % ZnO, 1.1 % FeO, 0.5 % Na_2O+K_2O, 0.2 % CaO, and 0.05 % Cl. The average and standard deviation of the various analyses made on the crystallites are shown in **Table I**. Type I crystals contain 86.1 wt. % Pb and 13.6 wt. % S and no O, corresponding to galena. Type II and Type III crystallites are identified by SR-μXRD as lanarkite, $PbO{\cdot}PbSO_4$, and mattheddleite, a lead silicate sulphate chloride[18-20] of composition $Pb_{10}(SiO_4)_{3.5}(SO_4)_2Cl_2$ respectively, as shown in *Figure 6*. The chemical composition obtained for the Type II crystals is also in good agreement with those of lanarkite, $PbO{\cdot}PbSO_4$. Conversely, the chemical composition determined for the Type III crystallites $(Ca_{0.04},Pb_{0.96})_{10}(SiO_4)_4(SO_4)_2Cl_{0.8}$, differ from the theoretical composition; contains less Cl, some unexpected Ca and unbalanced Si and S. In fact, mattheddleite is a rare mineral of the apatite supergroup (ellestadite) of theoretical composition $Pb_5(SiO_4)_{1.5}(SO_4)_{1.5}(Cl,OH)$[21]; the other endmembers of this group are hydroxylellestadite and fluorellestadite of theoretical composition $Ca_5(SiO_4)_{1.5}(SO_4)_{1.5}(OH)$ and $Ca_5(SiO_4)_{1.5}(SO_4)_{1.5}F$ respectively.[20] Consequently, calcium may also be incorporated in the structure. The unbalanced Si and S measured by EPM was already noticed and associated to large and inaccurate absorption corrections occurring when celestite is used as S standard[21]. In fact, our data is in good agreement with other mattheddleite EPM analysis. In our case, the neo-formed inclusions of mattheddleite integrated available elements from the surrounding environment (glaze) during crystallisation and, particularity incorporated some calcium. The gangue also included some sphalerite grains that explain the presence ZnO in the glaze.

Under the optical microscope (*Figure 7*) galena is easily recognizable in reflected light, *Figure 7c,* by its high reflectance and because of the fractures along the cubic planes of exfoliation of some grains. Lanarkite and mattheddleite can be distinguished with crossed polarized light (XPL); lanarkite displays 2nd /3rd order interference colours and inclined extinction (birefringence = 0.108), while mattheddleite has straight extinction and 1st and low 2nd order interference colours (birefringence = 0.018), *Figure 7b*. In addition, some tabular sections of lanarkite show polysynthetic twins. In reflected light, lanarkite shows relief and a darker contrast than mattheddleite, *Figure 7 (c)*.

The presence of different crystallites in the glaze is responsible for the various appearances and colours of the three areas: opaque green, translucent yellow and transparent honey. The occurrence of galena grains accounts for the opacity and the presence of Fe^{2+} ions dissolved in the glaze is most probably responsible for the green colour. The concurrence of galena and Fe^{2+} is explained by the glaze exposure to a reducing atmosphere during the firing. The shortage of oxygen is responsible for both, the delayed decomposition of galena and the reduction of the iron ions. A possible cause for this reducing atmosphere might be the exposure of the glazed surface to the flame. The opalescent-yellow and the transparent-honey areas would not have been exposed and, consequently, show the yellow tinge characteristic of Fe^{3+} and of lead glazes. Although both, lanarkite and mattheddleite crystallites are present in the opalescent yellow area, lanarkite crystallites are responsible for the opalescence, as they have a pearly lustre appearing macroscopically translucent. The transparent-honey area, however, contains only mattheddleite crystallites, which are transparent and show an adamantine lustre.

IV. Discussion

Although the first experimental studies of the PbO-SiO_2 system[9] indicated that a series of compounds with PbO:SiO_2 mole ratios of 4:1, 3:1, 2:1, 1:1, and 5:8 were formed; only $PbSiO_3$, Pb_2SiO_4 and Pb_4SiO_6 were confirmed by other research.[8,22] Moreover, Jak et al.[23] found that $PbSiO_3$ and Pb_2SiO_4 melt congruently while Pb_4SiO_6 decomposes incongruently. Our high temperature experiment is in perfect agreement with this. Moreover, the temperatures at which the different compounds form and decompose match our data, supporting the validity of our kinetic data.

On the other hand, based on the PbO-$PbSO_4$ phase diagram[13] for temperatures lower than 860°C, anglesite ($PbSO_4$) and lanarkite ($PbO \cdot PbSO_4$) are the two stable phases. Further oxidation tends to form lanarkite which leads to the subsequent development of first $2PbO \cdot PbSO_4$ and then $3PbO \cdot PbSO_4$.[24]

In the PbS-SiO_2 system studied, lead silicates are not formed. The lack of lead silicates is probably due to remaining sulphates in the glaze mixture that handicapped the crystallization of the PbO/SiO_2 compounds. The oxidation of galena gives rise mainly to the formation of lanarkite ($PbO \cdot PbSO_4$) at a temperature as low as ~315º C disappearing suddenly at 795º C. The sudden disappearance of lanarkite in the PbS-SiO_2 system happens at lower temperatures than in the PbO-$PbSO_4$ system. This can be related to the presence of SiO_2, which certainly plays a role, giving rise to a PbO-SiO_2 melt at ~775º C. The green and yellow areas of the misfired glaze also show the presence of a silica melt and lanarkite, but not the compounds formed at higher temperatures. Anglesite is often present in the original galena ore as a weathering product and, considering that it is stable up to ~860º C, it should be found in the misfired glaze. Therefore, absence of anglesite could be an indicative that it was not present in the galena used by ancient potters.

The two basic lead sulfates, $2PbO{\cdot}PbSO_4$ and $4PbO{\cdot}PbSO_4$ which are formed after the lanarkite decomposition in the high temperature experiment, are not found in the honey area of the historical lead glaze. In fact, the presence of both galena and lanarkite in the misfired glaze indicates not only a low firing temperature (below 795º C) but also a short firing. Moreover, the flame also produces a reducing atmosphere, which delays sulphur oxidation and sulphate decomposition. The green and yellow colours of the misfired areas also indicate the presence of reduced and oxidised iron respectively. Therefore, we can also suppose that the lack of oxygen due to the direct hit of the flame in the area affected the oxidation of galena and lanarkite and the formation of the glaze. Conversely, the transparent honey glaze shows neither galena nor lanarkite. However, mattheddleite $Pb_5(SiO_4)_{1.5}(SO_4)_{1.5}(Cl,OH)$, with some calcium substituting the lead atoms, is identified. Mattheddleite occurs in oxidized zones of lead deposits, associated with lanarkite and anglesite and its formation is driven by the presence of chlorine. The thin cross section shows the sequence of formation of the sulphate compounds in the glaze. Galena is found surrounded by lanarkite crystals, *Figure 7 (a)*, while lanarkite is found inside mattheddleite crystals in the green area of the glaze, *Figure 8*. Therefore, the sequence of compounds formed during the oxidation of galena is, first lanarkite and then mattheddleite, provided chlorine is available in the surrounding glaze.

There are two possible sources for the chlorine found in the glazes; it formed part of the galena mineral or there was contamination during the firing. A very popular lead mineral extraction site in Catalonia is the Begur Coast, also known as the coast of the six lead mines.[25] The mines are often flooded by seawater, which could explain the presence of chlorine in the galena gangue. On the other hand, the ashes generated burning halophyte type plants[26,27] during the firing could also provide chlorine to the surface of the glazes. In fact, the presence of ashes on the glaze surface during the firing could also explain the preferential direction of growth shown by the mattheddleite crystals –from the glaze surface towards the ceramic body- observed in the yellowish and honey areas of the glaze, *Figure 1(b,c)*.

The supposed disadvantage, initially considered based on the PbO-$PbSO_4$ phase diagram, of the high temperatures at which the decomposition of the lead sulphates and formation of a melt (~928º C) happen is not correct for the system PbS-SiO_2. Our data shows that in the system PbS-SiO_2 at a temperature as low as 775º C a melt is formed and that at 795º C the lanarkite is already fully decomposed. Nevertheless, adequate oxidation conditions are necessary to help the oxidative process take place. Consequently, optimal firing conditions for the PbS-SiO_2 system are a temperature only slightly higher than those of the PbO-SiO_2 system provided adequate oxidative conditions are guaranteed.

V. Conclusions

The transformations during the production of a lead glaze with galena PbS-SiO_2 were studied by means of a high temperature X-ray Diffraction experiment with Synchrotron Radiation (HT-SR-XRD). The phase transformations and thermal stability of the compounds formed were determined and the results obtained were compared to the available data for the PbO-SiO_2 and PbO-$PbSO_4$ systems. The oxidation of galena gives rise to the formation of lanarkite, $PbO{\cdot}PbSO_4$, at 315º C and its decomposition at

795°C, a temperature lower than those found in the $PbO-PbSO_4$ system (916º C). Moreover, in agreement with the $PbO-PbSO_4$ system, once lanarkite decomposes, two basic lead sulfates, $2PbO·PbSO_4$ and $4PbO·PbSO_4$ form. Lead silicates do not form in the $PbS-SiO_2$ system contrary to what is observed in the $PbO-SiO_2$ system where they form at temperatures above 750º C. The presence of lead sulphates in the silicate melt prevent the formation of the lead silicates. The results obtained show that the optimal firing conditions for the $PbS-SiO_2$ system are, a temperature rather similar to the $PbO-SiO_2$ system, but when galena is used, highly oxidative conditions need to be guaranteed in order to eliminate sulphur from the glaze.

A historical misfired lead glaze still retaining relics of galena was also studied and the crystalline phases developed were identified. Different colour areas - green, yellow and honey- showing different crystalline compounds of the glaze, were discussed. Galena, lanarkite, $PbO·PbSO_4$ and mattheddleite, $(Ca,Pb)_{10}(SiO_4)_{3.5}(SO_4)_2Cl_2$ were identified. The crystallites are responsible for the opaque green (galena, lanarkite and mattheddleite), opalescent-yellow (lanarkite and mattheddleite) and transparent-honey (mattheddleite) colours observed on the surface of the sample. The presence of galena and lanarkite indicates a maximum temperature of 795º C, although the reducing action of the flame could have delayed sulphur and sulphate oxidation even at higher temperatures. The crystallization of mattheddleite and its directional growth from the surface towards the glaze could be explained by the deposition of plant ashes on the glaze surface during the firing.

+

Acknowledgements

Roberta Di Febo is grateful to the UVIC-UCC Scholarship Program, awarded by University of Vic, Central University of Catalonia. The authors are grateful to the project MAT2016-77753-R, 2017-2019 funded by the Ministerio de Ciencia e Innovación (Spain) and the ALBA Synchrotron Light Facility 2014060905 (BL04). Thanks are due to the project 2014SGR00581 (T.P.), 2014SGR1585 (J.M. and R.D.F.) and 2014SGR1661 (J.C.M.).

References

[1]Tite MS, Freestone I, Mason R, et al. Lead glazes in antiquity- Methods of production and reasons for use. *Archaeometry.*1998: 40, 241-260.

[2]Wood N, Freestone I. A preliminary examination of a Warring States pottery jar with so-called 'glass paste' decoration. In *Science and technology of ancient ceramics: 3*. Proceedings of the international symposium on ancient ceramics. Edited by J. Guo. Shanghai Res. Soc. Sci. Technol. Ancient Ceram., Shanghai. 1995; 12-17.

[3]Wood N. Chinese Glazes, the origins, chemistry and re-creation. A&C Black London and University of Pensylvania Press, Philadelphia;1999.

[4]Walton M, Tite MS. Production technology of Roman lead glazed pottery and its continuance into late antiquity. *Archaeometry.*2010;52,733-759.

[5]Molera J, Pradell T, Salvadó N, et al. Lead Frits in Islamic and Hispano-moresque glazed productions. In From Mine to Microscope: Advances in the Study of Ancient Technology. Edited by A. J. Shortland, I. C. Freestone, T. Rehren. Oxbow Books. 2007; 11-22.

[6]Gómez A, Gil C, Di Febo R, et al. Casa Convalescència (Vic, Osona): Aproximació arqueológica i arqueomètrica a un conjunt de vasos ceràmics del segle XVIII. In *Actes*

III Jornades d'Arqueologia de la Catalunya Central, Publicacions Generalitat de Catalunya.2015; 70-81.

[7]Lessler MA. Lead and lead Poisoning from Antiquity to Modern Times. *Ohio J. Sci.* 1988; 88, 78-84.

[8]Geller RF, Creamer AS, Bunting EN. The system PbO-SiO_2, *J. Res. Nut. Bur. Stand.* 1934; 13, 237-244.

[9]Smart RM, Glasser FP. Compound Formation and phase equilibria in the system PbO-SiO_2. *J. Am. Ceram. Soc.*1974; 57, 378-382.

[10]Factsage, Phase diagram PbO-SiO_2.
http://www.crct.polymtl.ca/fact/phase_diagram.php?file=Pb-Si-O_PbO-SiO2.jpg&dir=FToxid

[11]Eric RH, Timucin M. Phase equilibria and thermodynamics in the lead-lead sulphide system. *J. S. Afr. Inst. Min. Metall.*1969; 88, 353-361

[12]Kullerud G. The lead-sulfur system. *American Journal of Science.*1969; 267, 233-256.

[13]Billhardt HW. New data on basic lead sulfates, *Journal of the Electrochemical Society*; 1970*;* 117, 690-692.

[14]Abdel-Rehim, A.M. Thermal and XRD analysis of Egyptian Galena*. Journal of the Thermal Analysis and Calorimetry.* 2006; 86, 393-401.

[15]Hammersley P, Svensson SO, Hanfland M, et al. Two-Dimensional Detector Software: From Real Detector to Idealised Image or Two-Theta Scan. *High Pressure Research.* 1996; 14, 235-248.

[16]Fauth F, Peral I, Popescu C, et al. The new Material Science Powder Diffraction beamline at ALBA Synchrotron. *Powder Diffraction*. 2013; 28, 360-370.

[17]Richemond WE, Wolfe, C. Crystallography of lanarkite. *Am. Min.*1938; 23, 799-804.

[18]Livingstone A, Ryback G, Fejer EE, et al. Mattheddleite, a new mineral of the apatite group from Leadhills, Strathclyde Region, *Scottish Journal of Geology.*1987; 23, 1-8.

[19]Steele IM, Pluth JJ, Livingstone A. Crystal structure of mattheddleite: a Pb, S, Si phase with the apatite structure. *Min. Mag.*2000; 64, 915-921.

[20]Pasero M, Kampf AR, Ferraris C, et al. Nomenclature of the apatite supergroup minerals. *European Journal of Mineralogy.*2010; 22, 163-129.

[21]Essene EJ, Henderson CE, Livingstone A. The missing sulphur in mattheddleite, sulphur analysis of sulphates and paragenetic relations at Leadhills, Scotland. *Min. Mag.* 2016; 70, 265-280.

[22]Calvert PD, Shaw RR. Liquidus behavior in the silica-rich region of the system PbO-SiO_2. *J. Am. Ceram. Soc*. 1970; 53, 350-352.

[23]Jak E, Degterov S, Wu P, et al. Thermodynamic Optimization of the Systems PbO-SiO_2, PbO-ZnO, ZnO-SiO_2 and PbO-ZnO-SiO_2. *Metall. Mater. Trans. B*. 1977; 28, 1011-1018.

[24]Ponsot B, Salomon J, Walter P. RBS study of galena thermal oxidation in air with MeV $^{16}O^{3+}$ ion beam. *Nucl. Instr. Meth. Phys. Res. B*. 1998; 136–138, 1074–1079.

[25]Perelló, JMM. Els minerals de Catalunya, Edited by Institut d'Estudis Catalans, Barcelona; 1990.

[26]Lynggaard F. Tratado de cerámica. Ediciones Omega, Barcelona; 1976.

[27]Misra M, Raglund K, Baker A. Wood ash composition as a function of furnace temperature. *Biomass Bioenergy*. 1993; 4, 103–116.

Figure Captions

Figure 1. The neck of a 18th century jar which exhibit a misfired glaze showing three colour glaze areas. SEM backscattering images of (A) the opaque green area which contains relics of galena (I) and neoformed crystallites II and III, (B) the translucent

yellow area containing crystallites II and III and, (C) the honey transparent area containing only crystallites III. (E) EDS spectra of the three types of crystallites.

Figure 2. High temperature XRD patterns (HT-SR-XRD) obtained during the firing of 70 wt. % PbO - 30 wt. % SiO_2. The XRD patterns corresponding to the initial mixture before heating (bottom) and after cooling (top) are also shown.

Figure 3. High temperature XRD patterns (HT-SR-XRD) obtained during the firing of the mixture 75 wt. % PbS – 30 wt. % SiO_2. The XRD patterns corresponding to the initial mixture before heating (bottom) and after cooling (top) are also shown.

Figure 4. Thermal stability ranges of the crystalline phases identified for (a) PbO-SiO_2 and (b) PbS-SiO_2. The ordinate axis is obtained from the intensity of the principal peak of each crystalline phase relative to the intensity of the MgO crucible, and gives a qualitative temperature evolution of each compound.

Figure 5. Selection of HT-SR-XRD patterns of the final firing stage for the mixture PbS-SiO_2.

Figure 6. SR-μXRD pattern of the crystallites in the misfired glazes. The reference patterns marked correspond to the JPDF database patterns 01-071-2069 for lanarkite and 00-041-0610 for mattheddleite.

Figure 7. OM images of the green area glaze. (a) PPL transmitted light showing opaque grains of galena (I), transparent crystals of lanarkite (II) and mattheddleite (III); (b) XPL transmitted light where the elongated section of the mattheddleite crystals shows a 1st order grey colour, the hexagonal basal sections are extinguished: the elongated and prismatic sections of lanarkite exhibit 2nd /3rd order interference colours; marked with

an arrow, a twin; (c) reflected light, galena (I) appears very reflectant, mattheddleite (III) exhibits lower relief than lanarkite (II); (d) XPL transmitted light with ¼ lambda compensator.

Figure 8. OM image in reflected light of a lanarkite crystallite inside a crystal of mattheddleite

Table 1. Average and standard deviation (in parenthesis) of the chemical composition of the crystallites measured by EPM. N number of crystallites measured. The oxygen is calculated by stoichiometry.

Wt%	N	Pb	S	Si	Cl	Ca	O	Sum
Type I	6	86.1 (0.3)	13.6 (0.1)	-	-	-	-	99.7 (0.3)
Type II	8	78.1 (0.8)	5.5 (0.1)	0.2 (0.2)	-	0.1 (0.1)	14.6 (0.2)	98.5 (1.1)
Type III	9	75.1 (0.5)	2.5 (0.1)	4.5 (0.3)	1.2 (0.2)	0.7 (0.1)	14.9 (0.2)	98.8 (0.3)

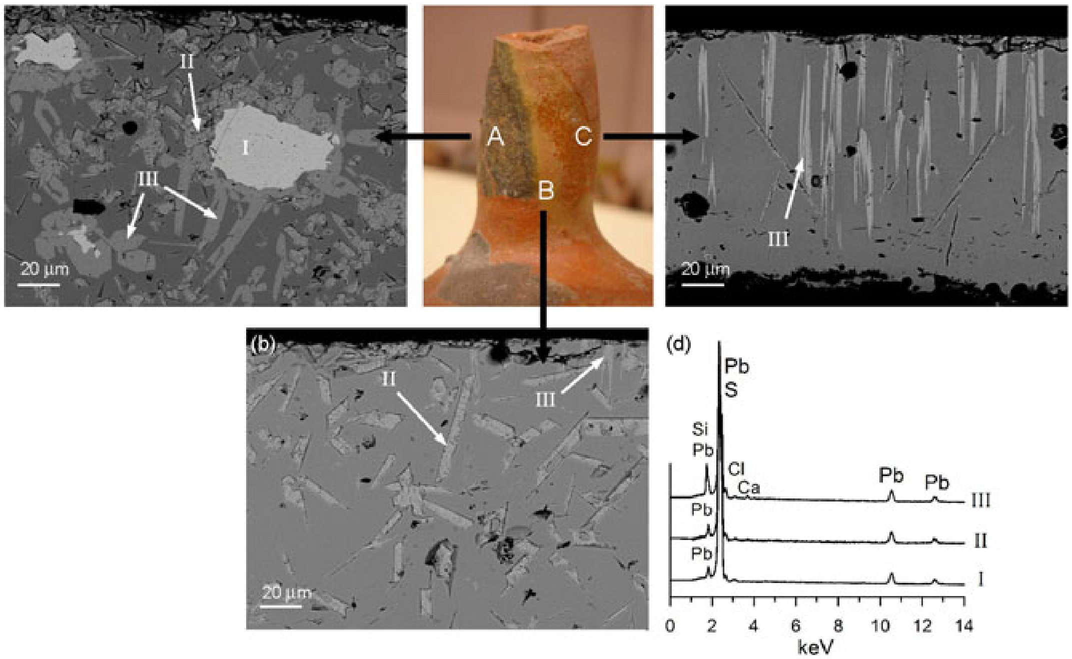

A
B
C
I
II
III
20 µm
(b)
(d)
Pb S
Si Pb
Cl
Ca
Pb
keV
0 2 4 6 8 10 12 14

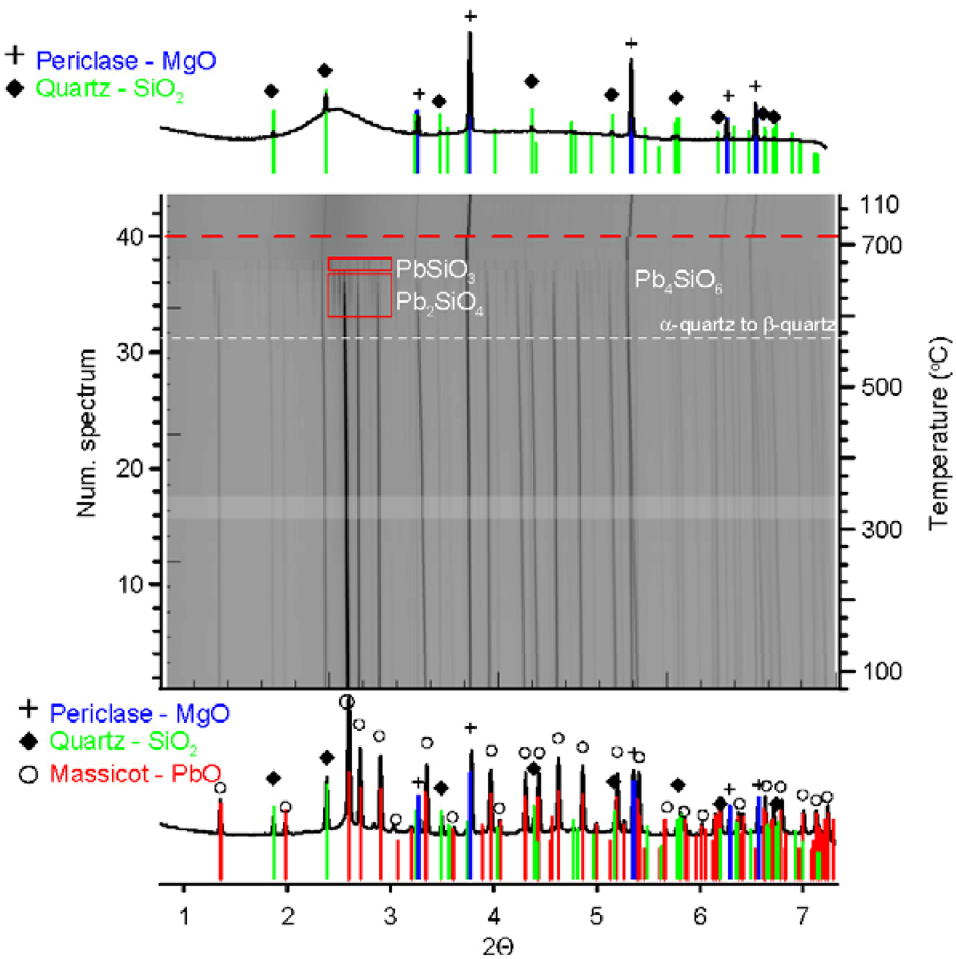

Periclase - MgO
Quartz - SiO2
Massicot - PbO
PbSiO3
Pb2SiO4
Pb4SiO6
α-quartz to β-quartz
Num. spectrum
Temperature (°C)
2Θ

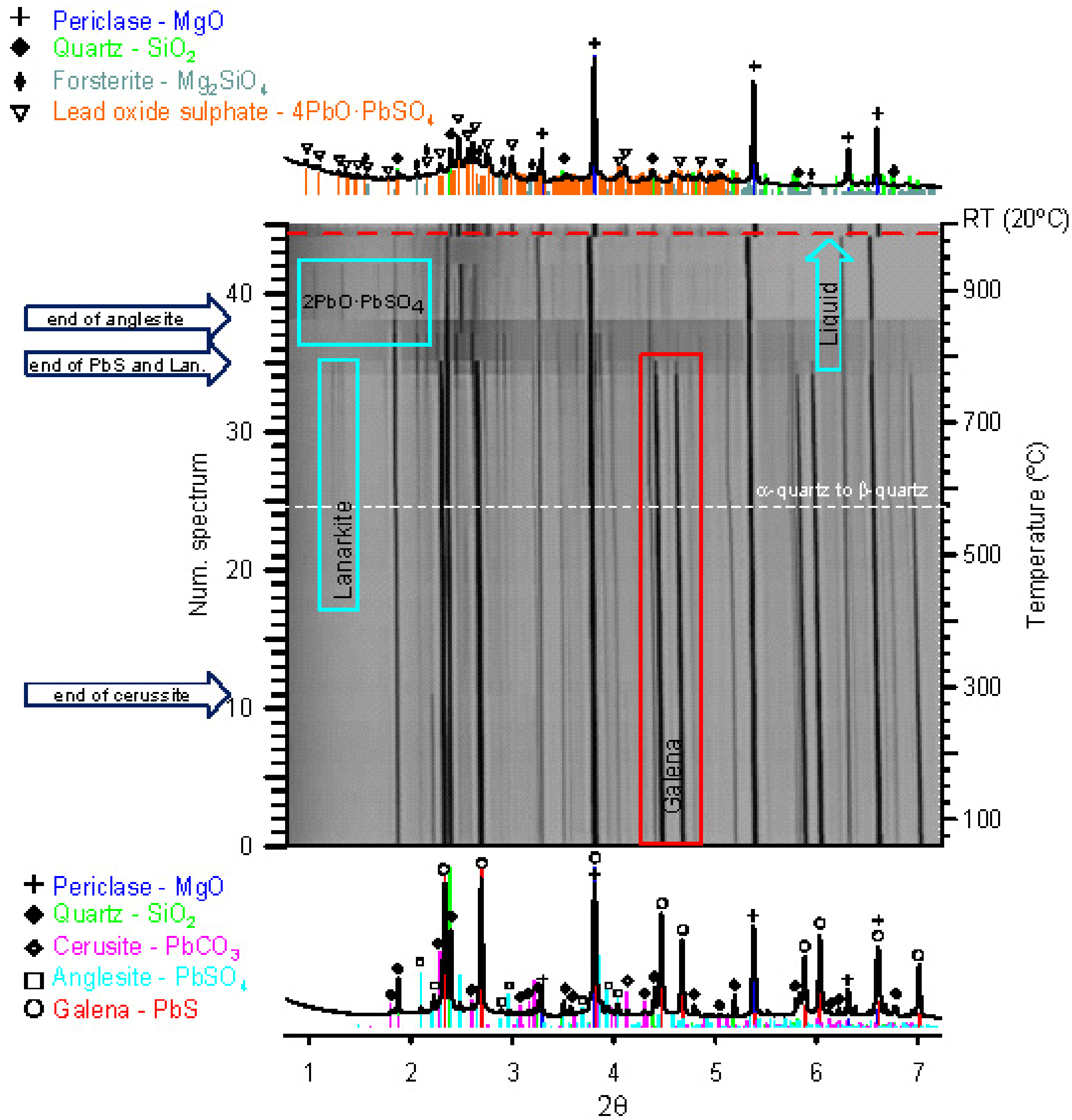

Periclase - MgO
Quartz - SiO_2
Forsterite - Mg_2SiO_4
Lead oxide sulphate - $4PbO \cdot PbSO_4$
RT (20°C)
$2PbO \cdot PbSO_4$
end of anglesite
end of PbS and Lan.
end of cerussite
Lanarkite
Galena
Liquid
α-quartz to β-quartz
Num. spectrum
Temperature (°C)
0
10
20
30
40
100
300
500
700
900
Periclase - MgO
Quartz - SiO_2
Cerusite - $PbCO_3$
Anglesite - $PbSO_4$
Galena - PbS
1
2
3
4
5
6
7
2θ

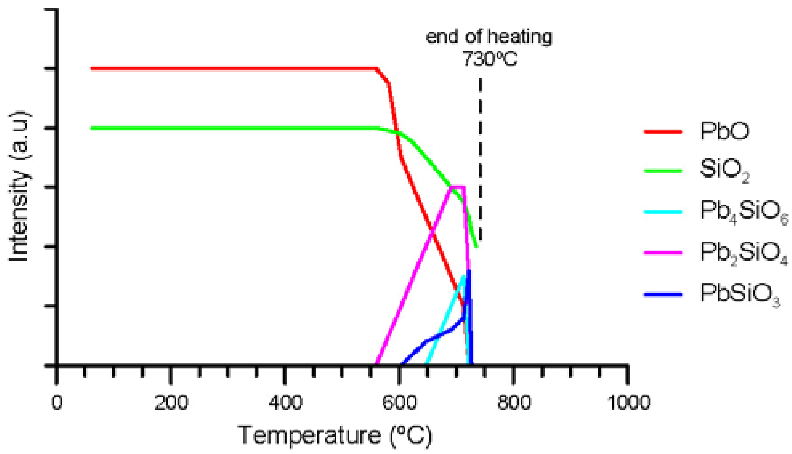
end of heating
730ºC
Intensity (a.u)
Temperature (ºC)
0
200
400
600
800
1000
PbO
SiO_2
Pb_4SiO_6
Pb_2SiO_4
$PbSiO_3$

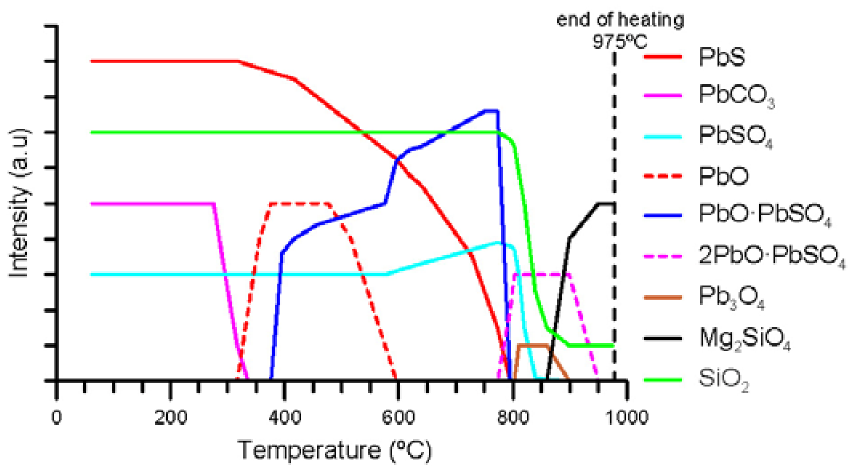
end of heating
975ºC
Intensity (a.u)
Temperature (ºC)
0
200
400
600
800
1000
PbS
$PbCO_3$
$PbSO_4$
PbO
$PbO·PbSO_4$
$2PbO·PbSO_4$
Pb_3O_4
Mg_2SiO_4
SiO_2

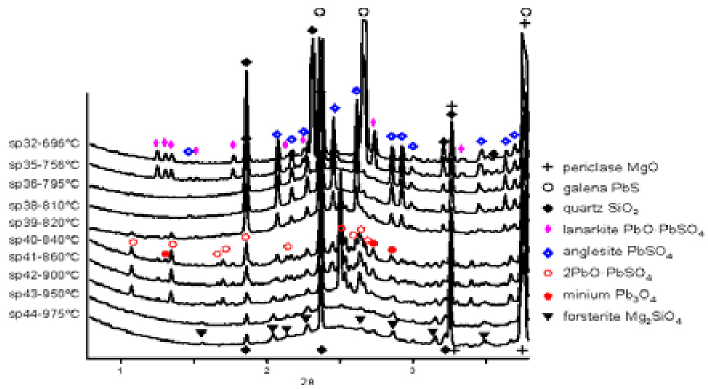
sp32-696°C
sp35-758°C
sp36-795°C
sp38-810°C
sp39-820°C
sp40-840°C
sp41-860°C
sp42-900°C
sp43-950°C
sp44-975°C
periclase MgO
galena PbS
quartz SiO_2
lanarkite PbO·$PbSO_4$
anglesite $PbSO_4$
2PbO·$PbSO_4$
minium Pb_3O_4
forsterite Mg_2SiO_4
1
2
3
2θ

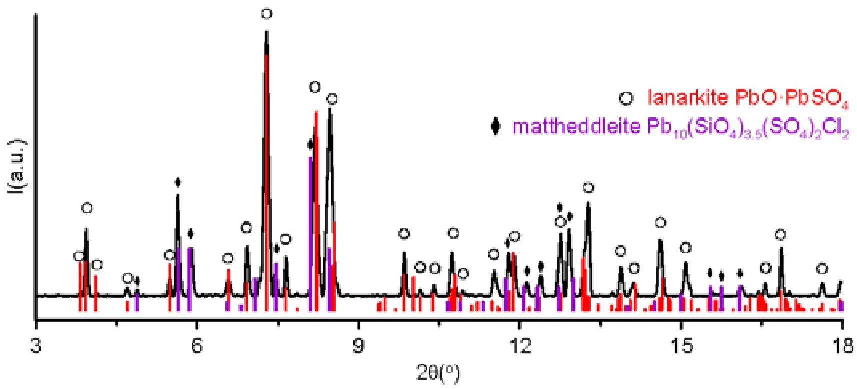
lanarkite PbO·$PbSO_4$
mattheddleite $Pb_{10}(SiO_4)_{3.5}(SO_4)_2Cl_2$
I(a.u.)
3
6
9
12
15
18
2θ(°)

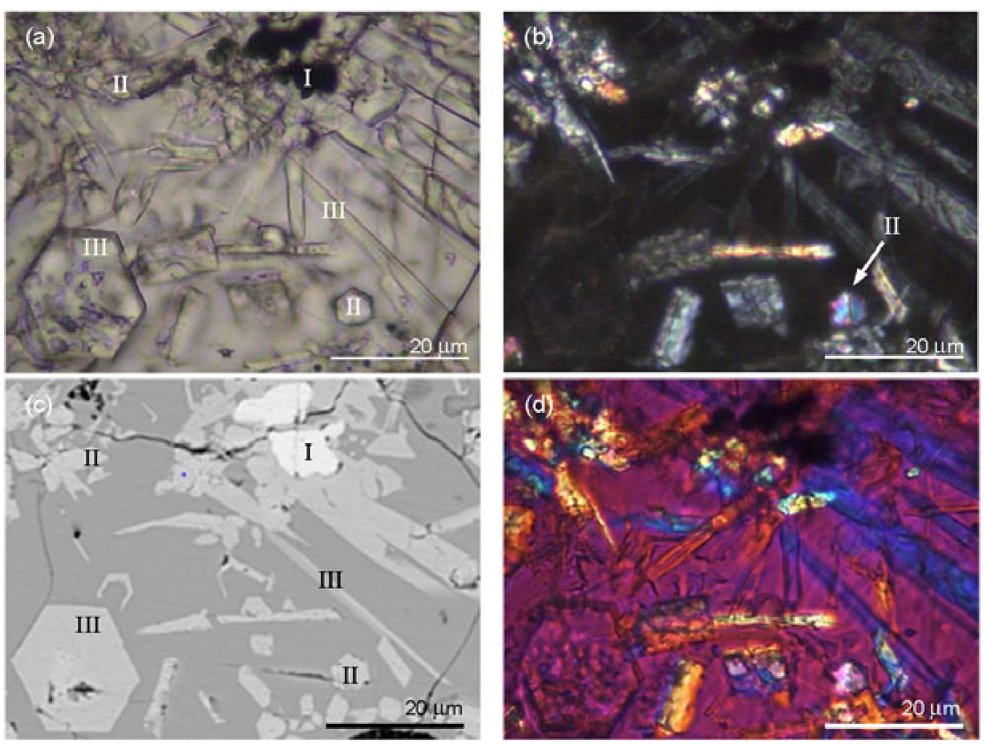
(a)
I
II
III
20 μm
(b)
II
20 μm
(c)
I
II
III
20 μm
(d)
20 μm

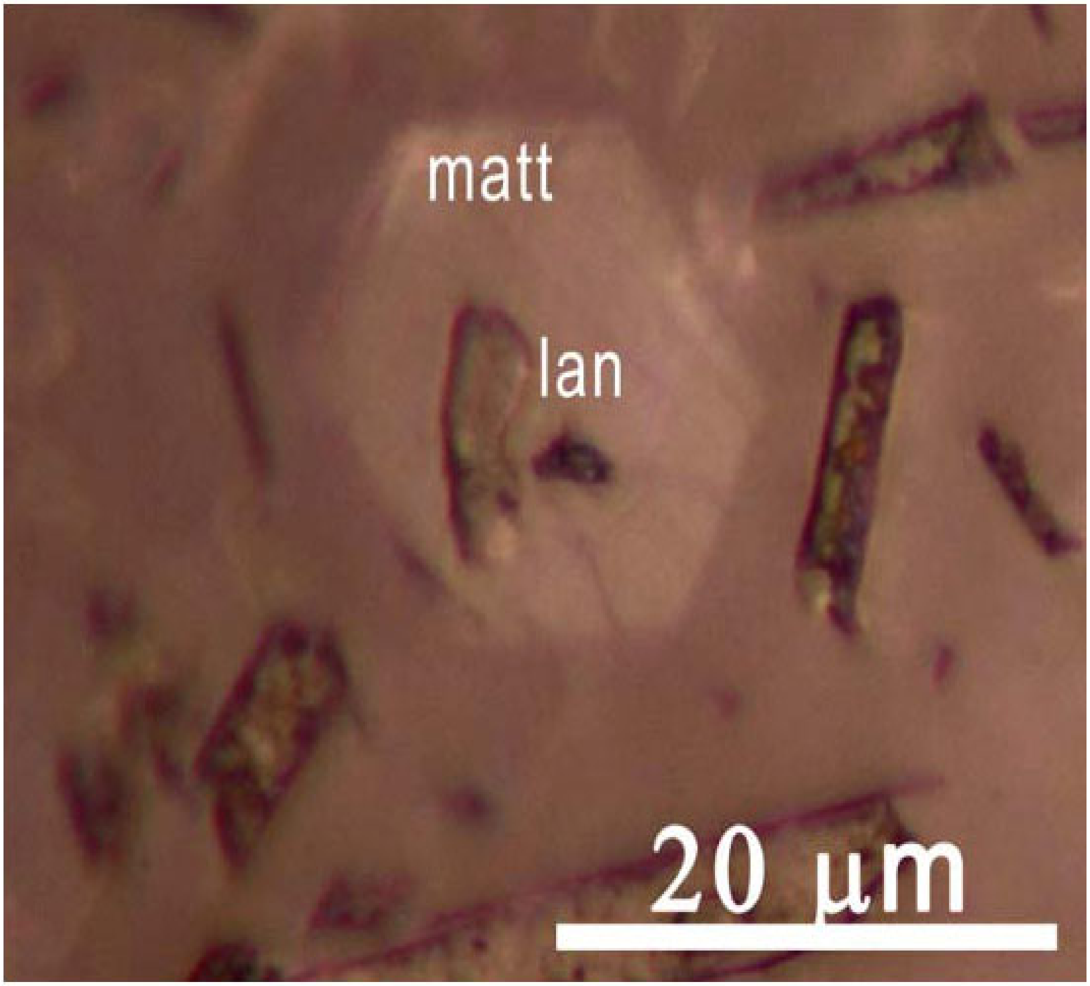
matt
lan
20 μm